Crack Propagation Fracture Toughness of Several Wood Species

Elijah Wilson, Meisam Shir Mohammadi, and John A. Nairn
Wood Science & Engineering, Oregon State University, Corvallis, OR, USA

Abstract

In materials with process zones, such as fiber bridging zones in wood, it is crucial to characterize fracture toughness as a function of crack growth, known as the material's *R* curve. Here, a new fracture testing protocol developed to measure continuous *R* curves was used on six different species of solid wood — Douglas-fir, Ponderosa pine, cedar, hemlock, balsa, and oak. Importantly, the new method uses monotonic loading, because unloading phases, as used in prior *R* curve methods, might damage the bridging fibers and alter subsequent toughness results. The crack length was recorded by a synchronized, automated imaging system. The solid wood *R* curves were measured for cracks running parallel to the wood grain direction with the crack plane normal to the radial direction (RL cracks) or normal to the tangential direction (TL cracks). The *R* curves for all species rose as a consequence of fiber bridging. TL toughness rose faster then RL toughness and therefore for long cracks TL toughness was higher for all species except cedar. The toughness trended upward as the density increased. Density had a much larger effect on fiber bridging effects (*i.e.*, the rise of the *R* curve) than it did on initiation toughness (*i.e.*, the start of the *R* curve).

Keywords: Fracture Toughness, *R* Curve, Wood, Fiber Bridging

Introduction

Many materials, such as wood [1], bone [2], concrete [3], and fibrous composites [4-6], develop process or damage zones in the wake of propagating cracks. A consequence of such zones is that the toughness changes as the crack propagates. In wood, which is the focus of this paper, the process zone is caused by unbroken wood fibers that bridge the crack surfaces. Because these fibers carry load, they cause the toughness to increase as the crack propagates. The dependence of toughness on crack growth is known as a material's fracture resistance curve or "*R* Curve." Such curves typically start at a low toughness, called the initiation toughness, and then increase as the process zone develops. Eventually the trailing edge of the process zone will fail. In wood, this failure occurs when the bridging fibers break and stop carrying load. Once this process zone failure starts, the zone is fully developed. Subsequent crack propagation will be by simultaneous crack tip propagation and process zone failure; *i.e.*, the process zone length will remain constant and propagate along with the crack [7]. In this stage the material will be at a constant steady-state toughness that is the sum of initiation and bridging zone toughness [8].

A complete characterization of wood toughness, *i.e.*, for any material with process zones, requires measurement of the full *R* curve. Such curves provide important fracture properties. The initial value defines a toughness to initiate failure. The rise in the curve defines the contribution of process zone mechanics to toughness or the absence of a rise indicates no process zone toughening mechanisms. If a region of constant or steady state toughness is reached, the plateau defines a long-crack-length toughness and the amount of crack growth required to reach steady state defines the size of the process zone. Unfortunately, traditional ASTM methods for measuring toughness do not measure an *R* curve, but instead focus on crack initiation. For example ASTM E-399 [9] creates an initial notch, observes the initiation of failure, and then calculates the toughness. This standard has been used on wood [10-15] and wood composites (*e.g.*, [15]), but because this method monitors initiation only, all such results are incomplete. Even as a measure of initiation, traditional fracture methods on wood are highly variable. The experiments give a single number that is prone to scatter. It is extremely difficult to use such fracture experiments to explain wood properties or to design wood structures to avoid cracking.

This paper describes a new testing protocol for measuring full *R* curves of wood [5-7]. In brief, wood specimens with an initial notch are loaded and both force and crack length are monitored as the crack propagates. When the specimens experience relatively stable crack growth, the experiments can be reduced to a continuous *R* curve. Two important considerations in wood are being able to accurately monitor crack length and being careful to avoid unloading steps that might damage the bridging fibers and alter subsequent propagation results. This new method, therefore, differs from prior *R* curve methods in fiber bridging composites that relied on unloading steps for calculation of incremental released energy (*e.g.*, [4]). When non-steady crack growth occurs, such as slip-stick propagation caused by anatomical features in wood, it is not possible to measure a continuous *R* curve, but it is still possible to get *R* curve results by discrete analysis of selected points along the crack growth process. This new testing protocol was used to characterize the fracture properties of six different wood species spanning a wide range in density and anatomy.

Besides the need to characters the full *R* curve in wood, wood is also an anisotropic material. The trunk of a tree is approximately cylindrically orthotropic. When cut into lumber, a board sufficiently far from the pith will be approximately planar orthotropic with three planes of symmetry having normal vectors in the radial (R), tangential (T), and longitudinal (L) directions of the original tree (see Fig. 1). Within each plane, crack propagation may be in the two other orthogonal directions. The standard fracture propagation nomenclature for these six crack-growth directions are defined by two letters, namely, RL, RT, TL, TR, LT, and LR, as illustrated in Fig. 1 [13,14]. The first letter is the direction of the normal vector for the crack plane while the second letter is the direction of crack propagation. Full characterization of wood fracture requires experiments in all crack paths, although LT or LR cracks cannot be studied for crack propagation

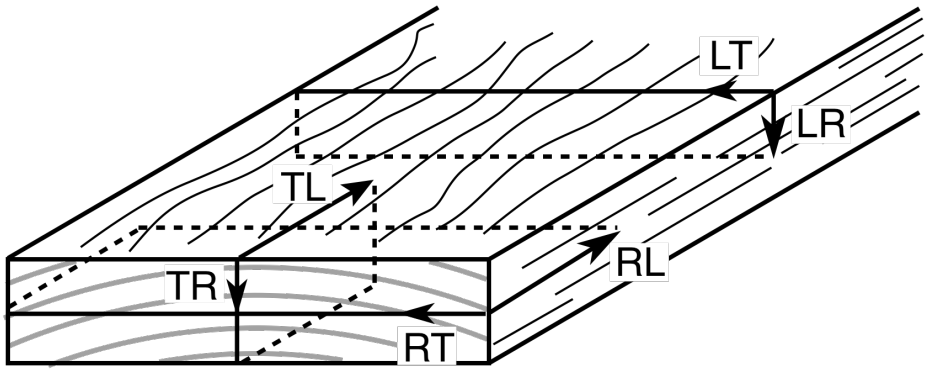

Figure 1: Standard nomenclature for fracture planes in wood. The first letter is the normal to the fracture plane and the second letter is the direction of crack propagation.

because such cracks always turn to become RL or TL cracks, rather than propagate as LT or LR cracks. Some experimental results claim to measure initiation toughness for LT or LR cracks [13,16], but because the initiation is not followed by propagation, those values are of questionable meaning. This paper is confined to RL and TL fracture (see Fig. 2). Both these crack paths are parallel to the wood fiber direction and therefore also the most likely to exhibit fiber bridging effects. RL crack planes are tangential to growth rings and therefore potentially have crack planes confined to one, or a few growth rings, and perhaps are dominated by crack growth within early wood layers. In contrast, TL cracks are perpendicular to the growth rings and therefore the crack front will always bridge across multiple growth rings and propagate in both early and late wood zones.

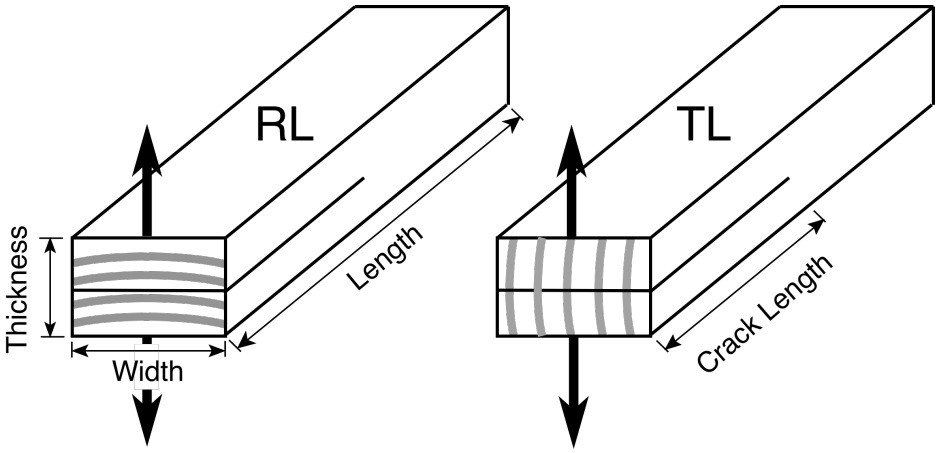

Figure 2: The mode I double cantilever beam (DCB) specimens used for RL fracture (left) and TL fracture (right). See text for specimen dimensions.

Materials and Methods

Six different species of solid wood were characterized for their fracture properties during crack propagation using the new method described below. The six species were Douglas fir *(Pseudotsuga menziesii*), Ponderosa pine *(Pinus ponderosa*), cedar *(Juniperus spp.*), hemlock *(Tsuga spp.*), balsa (*Ochroma pyramidale*), and oak (*Quercus spp.*). The first four are softwoods and the last two are hardwoods (although balsa is a low density and "soft" hardwood). Prior to testing, all specimens were stored in a conditioning room (20°C and 65% relative humidity) resulting in equilibrium moisture content for all specimens nominally at 12%.

This work measured mode I (tensile or opening mode) fracture for wood specimens propagating in the RL and TL directions by using double cantilever beam (DCB) specimens. The specimens were nominally of length, width and thickness of 400, 25, and 25 mm, respectively, with an initial crack length of 100 mm (see Fig. 2). The balsa specimens were 200 mm long and had an initial crack length of 75 mm. The initial cracks were cut down the center plane of each specimen with a narrow band-saw blade. Because all experiments focused on crack propagation, the initial crack preparation was not critical, provided it was sufficiently sharp to avoid overloading artifacts at initiation. The edge of the initial crack was cut wider for insertion of angle irons. The irons were gripped in an Instron 5443 testing frame; frictional contact between angle irons and wood specimens was sufficient to maintain loading. The arms were opened at 2 mm/min while recording force and displacement. The displacement near the load point was measured with an LVDT mounted on the specimen. All data were collected under ambient conditions soon after removal from the conditioning room. We did three replicates for each species and each crack orientation. After each test, specimen densities for regions near the crack tip were measured to investigate the effect of density on fracture toughness.

A key challenge for fracture experiments with solid wood (as well as both wood composites and non-wood composites) is accurate determination of the crack length. In these experiments, an automated camera system took periodic pictures synchronized with time stamps corresponding to force-displacement data. We were able to measure crack lengths by careful observation of the synchronized images. Correct determination of crack tips required practice and experience. When in doubt, subsequent images could be viewed to verify which features corresponded to crack propagation and which were anatomical feature in the wood, by observing how they changed between images. Accurate and correct determination of crack length is crucial to the data analysis.

Proposed Crack Propagation Fracture Energy Testing Protocol

The *R* curve method used here was based on the method introduced in Ref. [7] and used in Matsumoto and Nairn [5,6]. The experimental task is to record force and crack length as a function of displacement, which can be achieved by methods described above. Importantly, these

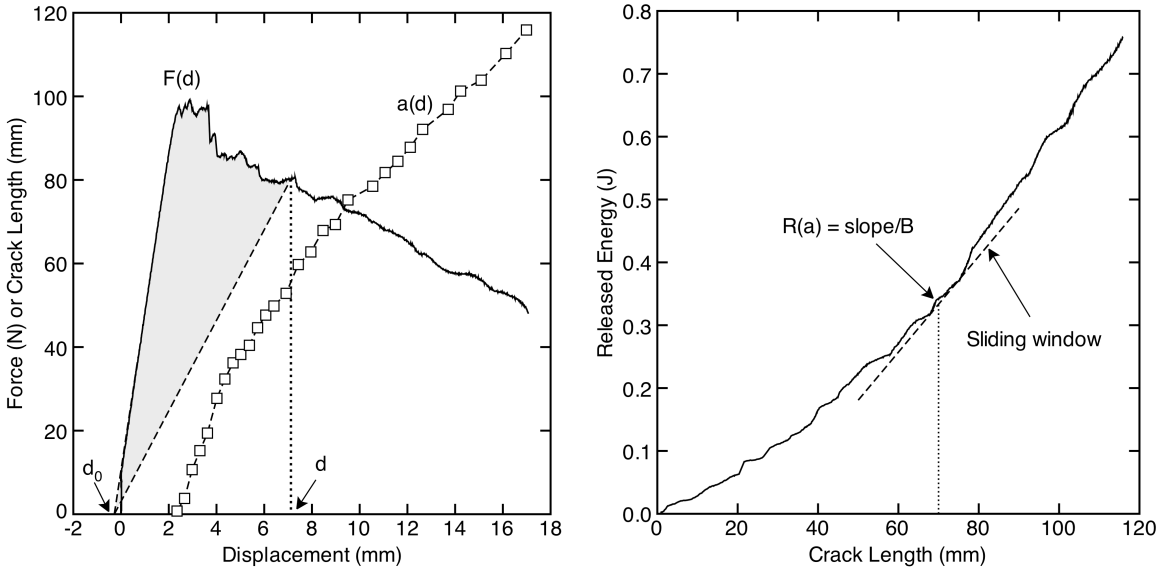

Figure 3: Area method for direct calculation of R curve from synchronized force and crack length data as a function of displacement. A. Force and crack length data. The shaded area is the area under the force-displacement curve from origin (d_0) to displacement d. B. Plot of the shaded area in A as a function of crack length at the corresponding displacement.

experiments have to be done during monotonic, continuous loading. Although *R* curves have been measured in some materials by a sequence of loading and unloading experiments [4], that approach is not advisable in wood [5]. In wood, the process zone can be large and filled with fibers bridging the crack plane. If specimens were unloaded during testing, that unloading would crush the fibers and possibly alter subsequent fracture properties.

Once force, displacement, and crack length data are recorded, the data are reduced as follows. Figure 3A shows sample force and crack length as a function of displacement from one experiment on hemlock. The shaded area under the force-displacement curve is a calculation of cumulative energy released up to a given displacement, *d*. This calculation requires knowledge of how the specimen unloads from *d*. If one tried to measure the return line by unloading, the fiber-bridging zone would interfere with the unloading and not return to the origin (*i.e.*, the fibers would not slide back into their original location and would likely be crushed instead). But any energy associated with such crack plane interference during unloading is not part of the energy released during monotonic crack propagation and therefore should not be part of the calculated cumulative released energy [17]. Instead, this protocol *assumes* that in the absence of crack plane interference, the unloading would return to the origin (d_0, found by extrapolation of the initial linear loading region to zero force) and thus cumulative released energy, $U(d)$, is defined by:

$$U(d) = \int_{d_0}^{d} F(x)\, dx - \frac{1}{2} F(d)(d - d_0) \tag{1}$$

which is the shaded area in Fig. 3A. This approach is valid for any elastic material where energy released is due only to crack growth and process zone damage. If a material has significant inelastic deformation (such as for green wood), the method would need to be revised. We have two experimental results that suggest it is acceptable for dry wood fracture testing. First, one can load a specimen until some crack growth, maintain load while removing the bridging fibers with a shape knife, and then unload. The goal is to see how the material would unload in the absence of crack-plane interference. Such experiments were done on wood composites [5] and they showed an approximate return to the origin in the absence of that interference. Second, we could hypothesize unloading curves for oak, as discussed further below.

The next step is to cross-plot $U(d)$ against the crack length at the corresponding displacement or $a(d)$ to get $U(a)$. A sample $U(a)$ curve is shown in Fig. 3B. The energy release rate as a function of crack length, or R curve, is the slope of $U(a)$:

$$R = \frac{1}{B}\frac{dU(a)}{da} \tag{2}$$

where B is specimen width. The R curve for these sample data is the starred curve in Fig. 5 (which has other curves discussed below). As is typical for R curves in materials with process zones, the R curve rises as a function of crack length. This rising R curve is apparent in the $U(a)$ plot (Fig. 3B) by its positive concave shape.

With high-quality data and consistent crack propagation, the above process is easily automated. We developed a custom Java application for all calculations. The force-displacement data consisted of a large number of data points and was easily integrated. Crack length was measured at selected displacements during the test and then found at other displacements by interpolation. Several interpolation schemes (piecewise linear, spline interplant, *etc*.) were tried; all worked well if crack data were sufficiently smooth. The hardest phase of the analysis is numerical differentiation of $U(a)$ (Fig. 3B). Again several methods were used. The most reliable method was to use linear fits to a sliding window (of user-adjustable size) along the data. The R value for the crack length at the center of each window is found from the slope of that window's fit (see Fig 3B). For each experiment, we tried various window sizes to verify R curve reliability. With good data, R curve shapes were independent of sliding window size, although smaller window sizes eventually picked up local variations in energy leading to noisier R curves.

The above analysis assumes that once a crack initiates, its propagation in sufficiently stable and continuous. Although DCB specimens of homogeneous materials under displacement control are predicted to have stable, continuous crack growth, wood is not a homogeneous material. Fortunately, all specimens except oak had sufficiently stable crack growth and could be analyzed by the method above. For oak, however, the crack propagation proceeded by a slip/stick process. A sample force-displacement curve for oak is shown in Fig. 4. Instead of a monotonic drop in force after the peak force, the force periodically dropped and then increased

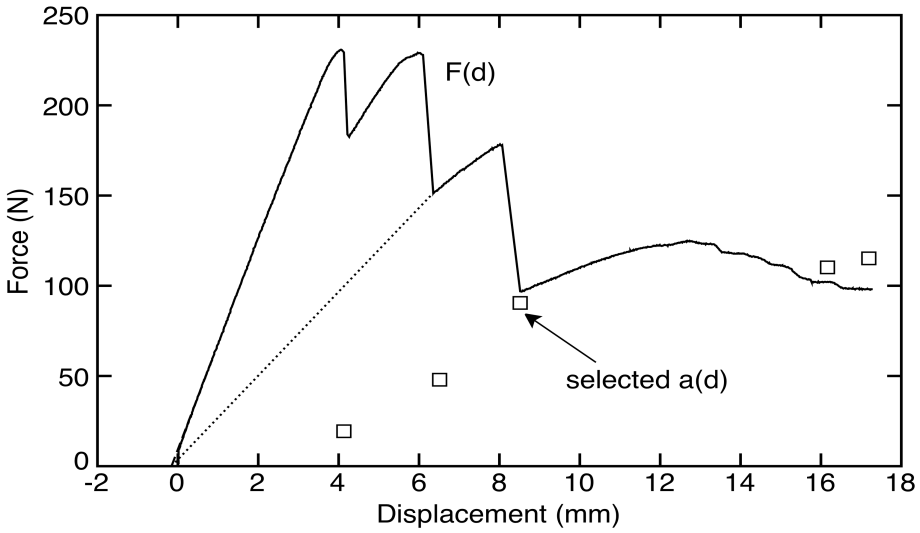

Figure 4: A typical force-displacement curve for an oak specimen, which is a species that had slip-stick crack propagation. The crack lengths (symbols) were recorded after each drop in load, because drops were observed to correspond to an increment in crack length. The dotted line shows that extrapolation of intermittent loading is consistent with unloading approximately to the origin.

before the next drop. The drops corresponded to increases in crack length. The increasing regions corresponded to loading with little or no crack growth. Our only option for analysis of oak (or analogous results for similarly behaving materials) was to use a discrete analysis. Instead of finding continuous crack length results, we recorded selected crack lengths at displacements corresponding to known crack propagation phases, such as soon after each load drop (see symbols in Fig. 4). Then, for each adjacent pair of crack length results, the energy release is found from

$$R = \frac{1}{B}\left(\frac{U(d_{i+1}) - U(d_i)}{a(d_{i+1}) - a(d_i)}\right) \tag{3}$$

and assigned to the toughness for mean crack length $(a(d_{i+1})+a(d_i))/2$. Here $U(d)$ is still found by Eq. (1) and therefore calculations were easily added to the Java application by replacing the slope calculation in Eq. (2) with the discrete calculation for adjacent pairs of provided crack length data in Eq. (3).

The slip-stick nature of crack propagation in oak, allowed us to hypothesize an unloading path. After each load drop, the load increased until the next crack propagation. As indicated by the dotted line in Fig. 4, extrapolation of these increasing segments back to the origin is consistent with an unloading process that returns to the origin. This observation is additional experimental evidence that unloading of wood in the absence of crack plane interference would return to the origin. In other words, the slope while increasing load at constant crack length approximates the unloading stiffness in the absence of crack plane interference that should be

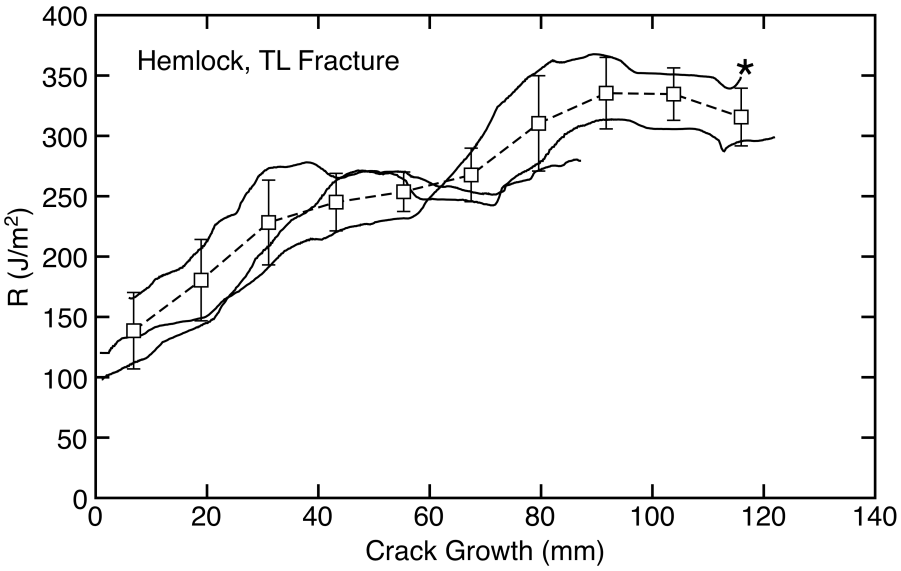

Figure 5: The solid lines are three experimental R curves for TL fracture in hemlock. The starred curve is the R curve calculated from the raw data in Fig. 3. The dashed curve is an averaged R curve using 10 boxes of crack length data. The error bars are standard deviations of the results in each box.

used for released energy calculations. The slightly lower slope while loading compared to slope of the dotted line could be a consequence of some crack growth during loading, *i.e.*, not exactly constant crack length loading.

Results and Discussion

Individual Specimen Results for Hemlock

The measurement and averaging of *R* curves for one species is presented first. Figure 5 shows results for TL fracture of three individual specimens of hemlock. The starred curve is the *R* curve resulting from raw data in Fig. 3; the other two curves are results for two more specimens. As is characteristic of *R* curves for materials with process zones, namely fiber bridging in wood, the *R* curve starts low and then rises. In hemlock, the *R* curves started at 100 to 150 J/m^2 and rose after 100 mm of crack growth to 300 to 350 J/m^2. In other words, after some crack growth, the toughness of hemlock is determined more by the fiber bridging than the initiation toughness. When prior work on wood fracture has focused on initiation only (*i.e.*, use of fracture mechanics standards), that work ignores fiber bridging and therefore misses important characteristics of wood toughness.

The rising portion of the *R* curve is an indication of the extent of the fiber-bridging zone. For hemlock, the fiber-bridging zones in DCB specimens are at least 100 mm in length (note: process zone lengths are specimen dependent and not a material property), which is large compared to many other materials studied by fracture mechanics (*e.g.*, bone [2]). When process zones are

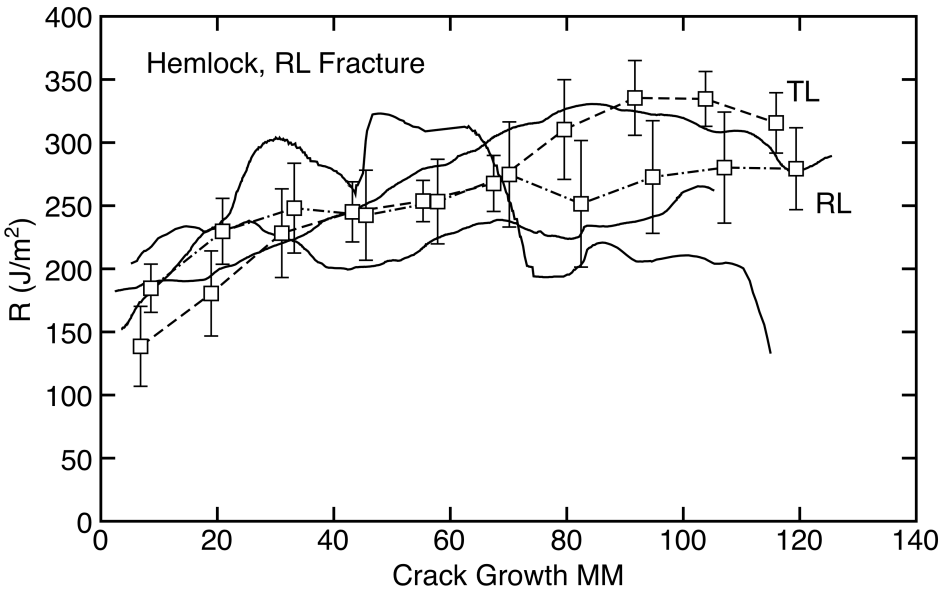

Figure 6: The solid lines are three experimental R curves for RL fracture in hemlock. The dash-dot curve is an averaged R curve using 10 boxes of crack length data. The error bars are standard deviations of the results in each box. The dashed curve is the averaged R curve for TL fracture re-plotted from Fig. 5 for comparison.

fully developed, the *R* curve should level off at a steady state value. It is possible that steady state was reached in hemlock at 300 to 350 J/m^2 after 100 mm of crack growth. Our specimens were limited to about 100 mm of crack growth. A better observation of steady state propagation would require longer DCB specimens. A consequence of very large process zones is that their properties are relevant to real-world applications. For example, process zones may be comparable in size to large, structural wooden beams. The propagation of cracks in such beams will be controlled more by the late stages of the *R* curve than by the initiation. In other words, crack propagation energy experiments are crucial to evaluation of fracture properties relevant to large beams. In contrast, standard fracture mechanics tests based on initiation of failure will not correlate well with real world performance.

A drawback of measuring *R* curves as opposed to a single number is that curves are more difficult to average and tabulate. To find an average curve, we divided the crack growth space into boxes of fixed width (*e.g.*, 10 mm), collected all results that fell within each box, and then averaged those results. The dashed curve in Fig. 5 shows the average *R* curve calculated from the individual specimens curves. The error bars are standard deviations of data within each box.

Figure 6 shows the analogous results for RL fracture of hemlock along with its averaged curve. The initiation toughness was about 150 to 200 J/m^2. The *R* curve increased and appeared to reach a steady state value of about 250 J/m^2 after about 80 mm of crack growth. The average *R* curve for TL fracture is included in Fig. 6 for comparison to RL fracture. The RL toughness is slightly higher at initiation, but the increase in toughness is larger for TL fracture. For long crack

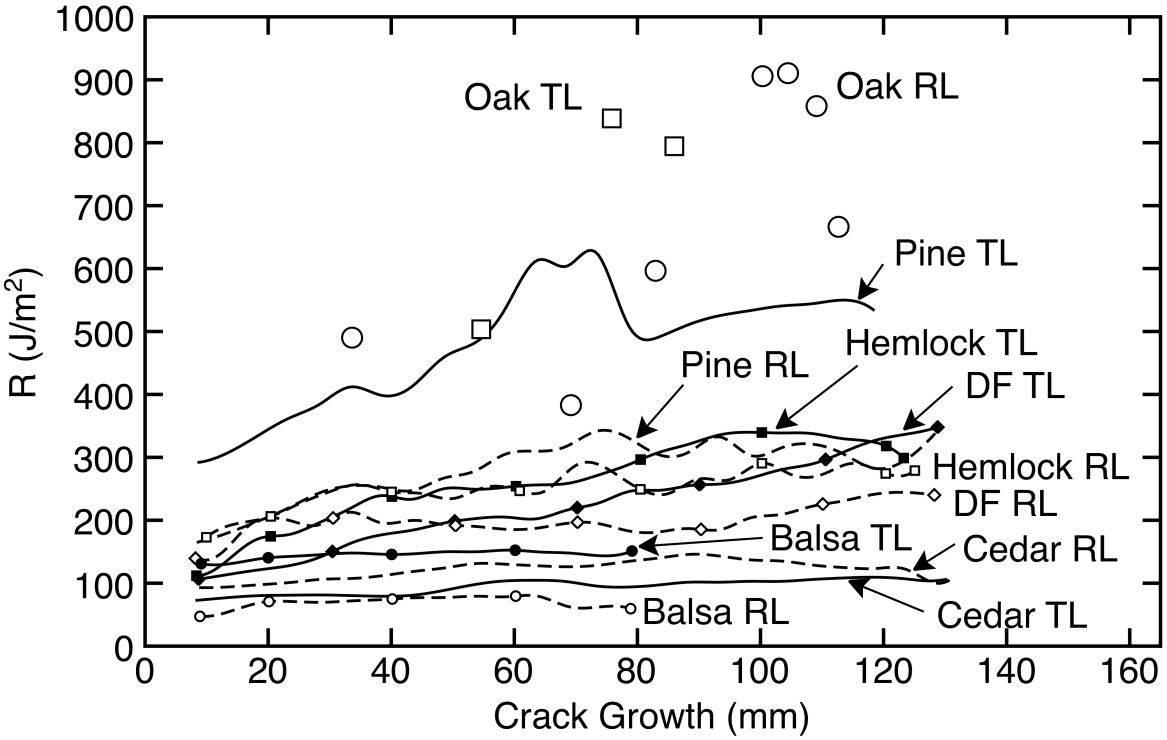

Figure 7: The fracture resistance, or R curves, for six species of wood as a function of the amount of crack growth. Each curve is an average of two or three separate R curves. The solid lines are for TL fracture and the dashed lines are for RL fracture. The small symbols are used to help distinguish the curves with solid symbols for TL curves and open symbols on RL curves.

lengths, the TL toughness is higher. Another drawback of *R* curves, as opposed to a single toughness number, is that it is more difficult to compare curves than single numbers and curves sometimes cross, giving mixed results. The advantage of full *R* curves is that they provide more fracture characterization information. The results for hemlock suggest that RL cracks, because of their lower toughness at long crack length, will be more damaging in beams and would be more likely to propagate to longer lengths eventually leading to degradation in beam properties. Such information could not be deduced from prior fracture test methods.

Average Curves for All Species

Figure 7 shows average *R* curves for all species tested. Each curve is an average of two or three individual specimens (usually three). The standard deviation error bars on the averages were omitted for clarity; the magnitudes were similar to the bars in Figs. 5 and 6. The solid lines are for TL fracture and the dashed lines are for RL fracture (the small symbols are used to help distinguish the curves). Because the balsa specimens were shorter, the experiments had less amount of crack growth. The balsa specimens also had shorter initial crack length, but all data are plotted as crack growth, which is total crack length minus the initial crack length. The results for oak failed by slip-stick crack propagation and therefore could not be analyzed for a

continuous R curve. Instead, we used the discrete method (Eq. (3)) to evaluate R curve at selected points after known crack propagation, as indicated by large symbols.

All R curves rise as a function of crack growth, but the extent of rise varies widely. The lower toughness species, balsa, cedar, and Douglas fir in the RL direction, barely increased (by less than 60 J/m^2), indicating fiber bridging plays a smaller role in these species. All other R curves increase by more than 100 J/m^2 and pine in the TL direction increased by over 300 J/m^2. For these species, fiber bridging has a dominant role in the crack propagation properties. Oak has the highest toughness and possibly the largest fiber bridging effect, but when only discrete experiments are possible, the resulting R curve is less accurate. The next sections evaluate the role of RL *vs*. TL fracture and the effect of density.

RL vs. TL Fracture

Several prior studies have compared RL toughness to TL toughness. Since these methods have relied on conventional fracture mechanics methods (e.g., ASTM E-399 [9]), which we argue provide only partial evaluation of fracture properties, the conclusions are, not surprisingly, varied. Schniewind, and Centeno [13] used conventional fracture mechanics on Douglas fir and found RL toughness to be higher than TL toughness. They concluded the differences were significant and "could be attributed to rays acting as crack arrestors in the RL system, while in the TL system the cracks can run along the rays." Ray cells are radial cells in wood involved in water transport [18]; they would be normal to the crack surface of RL cracks, but parallel to the surface in TL cracks. In contrast, Johnson [14] found RL toughness of Douglas fir to be slightly lower than TL toughness, but stated the results for these two directions were indistinguishable. Frühmann *et al*. [19] used wedge specimens and a "total work of fracture" method and found TL toughness higher than RL toughness in both spruce and beech. They concluded that late wood material enhanced the TL toughness. Reiterer *et al*. [20, 21] used similar specimens, but observed RL toughness higher than TL toughness in spruce, alder, oak and ash. They attributed the difference to ray cells, particularly in the hardwood species (where ray cells are larger [18]). In short, results based on incomplete fracture information vary, even in the same species (Douglas fir and spruce). Any result can even be explained by wood anatomy — when RL toughness is higher, it is because of ray cells; when TL toughness is higher, it is because of late wood fibers.

Some new trends in RL *vs*. TL fracture emerge when observing the entire R curves in Fig. 7. For long cracks (*i.e.*, after 70 to 100 mm of crack growth), TL toughness is higher in every species tested except for cedar (and the results for oak are indeterminate due to only having scattered R curve points). The results for initiation, however, are more varied. Either RL or TL may be higher and they are indistinguishable for some species. The TL toughness is usually higher at long crack length because the R curves for TL fracture have a higher slope than the R curves for RL fracture. This observation is most clear for Douglas fir where the RL toughness is

Table 1: The densities of each species and each specimen type measure in the path of the crack propagation. The numbers are averages for each specimen type.

Species	**RL** (g/cm^3)	**TL** (g/cm^3)
Balsa	0.246	0.273
Cedar	0.352	0.344
Douglas fir	0.447	0.527
Hemlock	0.450	0.350
Pine	0.475	0.491
Oak	0.698	0.692

nearly constant while the TL toughness more than doubles with crack growth. These differences agree with prior crack propagation experiments on Douglas fir [6]. Our conclusions are that RL and TL initiation toughness are similar in most species (with balsa and pine being exceptions), but that fiber bridging plays a much larger role in TL toughness as the crack propagates. This conclusion follows from a connection between high slope and more fiber bridging. Presumably the enhanced fiber bridging is due to higher proportion of higher-density late wood fibers bridging TL cracks than would be available for RL cracks.

Effect of Density

Many wood properties are affected by density. A qualitative analysis by Gibson and Ashby [22], based on cellular mechanics, claims that toughness, as stress intensity factor K_{IC}, should scale as density squared for low-density woods and as density to the 3/2 power for higher density woods. Because R or energy release rate is the square of stress intensity factor, this model predicts toughness will scale as density to fourth for low-density woods and density cubed for higher density woods. To check this scaling claim and to look at other affects of density, we recorded the densities of all fracture specimens. The average density values for each specimen type are given in Table 1.

To see scaling effects, two features of the R curves are given in

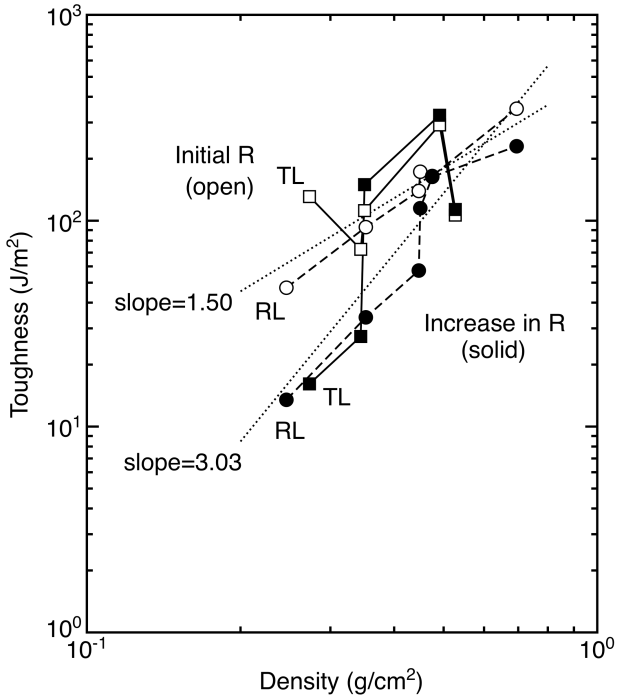

Figure 8: Selected R curve properties as a function of specimen density. The open symbols are the initiation toughness or initial R value and the filled symbols are the increase in toughness up to 70 mm of crack growth. The circles are for RL toughness and the squares are for TL toughness. The dotted lines are power low fits (with indicated slopes) to all initial toughness or toughness increase results, respectively.

a log-log plot as a function of density in Fig. 8. The initial *R* values (open symbols) show the initiation toughness as a function of density. The initiation of oak was estimated only for RL toughness to be about 350 J/m^2. The trend is positive indicating an increase in toughness as density increases, but the increase is much slower than predicted by Gibson and Ashby [22]. A log-log fit to all initiation data has a slope of 1.50 instead of the predicted 3 to 4. In general, the variations between species are similar in magnitude to variations due to density (*i.e.*, the scatter around the trend line).

Density plays a larger role in the fiber bridging effect, which was quantified here by plotting the change in toughness between initiation and the toughness after 70 mm of crack growth (see solid symbols in Fig. 8). The toughness increase for oak was estimated only for RL toughness to be about 230 J/m^2. The lowest density species, balsa and cedar, had nearly flat *R* curves, while the increase for higher-density species was much larger such that their toughness after significant crack propagation was dominated by fiber bridging effects. A log-log fit to all toughness increase results has a slope of 3.0. Although this slope is closer to Gibson and Ashby [22] scaling, it cannot be used as validation of their analysis, because their analysis did not consider fiber bridging. They claimed to be modeling cell wall breaking (at low density) and cell wall peeling (at high density).

Conclusions

When materials develop process zones during crack propagation, it is essential to record their crack propagation *R* curve rather then confine experiments to standard fracture mechanics tests for fracture initiation. Furthermore, when process zones take a long time to develop (*i.e.*, a distance comparable to specimen dimensions), the need for crack propagation experiments increases. Wood is such a material with a process zone characterized by fiber bridging, especially when crack growth is along the wood grain. This paper describes a new protocol for measurement of a complete *R* curve in fiber-bridging materials from a single experiment using monotonic loading and digital imaging to simultaneously track crack length. Furthermore, the experiments have to be done with monotonic loading because any unloading during the test (*e.g.*, to monitor unloading stiffness) would likely damage the process zone and alter the subsequent *R* curve. The test method works well whenever relatively continuous crack propagation occurs and sufficiently accurate crack lengths can be determined. For wood species with slip/stick crack growth, due to anatomical features, selected points can be used to find discrete points along the *R* curve.

This work looked at six different species of solid wood and characterized their fracture properties during crack propagation for both RL and TL cracks. The initiation values in RL and TL were usually similar, but the increase in toughness was always larger for TL fracture then for RL fracture. A toughness increase is associated with fiber bridging effects and therefore fiber

bridging by late wood fibers probably accounted for the larger effect in TL toughness. Both initiation toughness and the increase in toughness due to fiber bridging increase with wood density. Density has a much larger affect on fiber bridging than on fracture initiation.

Acknowledgements

This work was funded in part by the Wood Based Composites Center, an NSF I/UCRC, Grant 1034975, and in part by 3A Composites, Switzerland.

References

1. Smith, I., and Vasic, S., 2003,"Fracture Behaviour of Softwood," Mechanics of Materials, Vol. 35, No. 803–815.
2. Nalla, R. K., Kruzic, J. J., Kinney, J. H., Ritchie, R. O., 2005, "Mechanistic Aspects of Fracture and R-curve Behavior in Human Cortical Bone," Biomaterials, Vol. 26, pp. 217-231.
3. Li, V. C., Chan, C.-M., and Leung, C. K. Y., 1987, "Experimental Determination of the Tension-Softening Relations for Cementitious Composites," Cement and Concrete Research, Vol. 17, pp. 441–452.
4. Hashemi, S., Kinloch, A. J., and Williams, J. G., 1990, "The Analysis of Interlaminar Fracture in Uniaxial Fibre Reinforced Polymer Composites," Proc. R. Soc. Lond., Vol. A347, pp. 173–199.
5. Matsumoto, N. and Nairn, J. A., 2009, "The Fracture Toughness of Medium Density Fiberboard (MDF) Including the Effects of Fiber Bridging and Crack-Plane Interference," Engr. Fract. Mech., Vol. 76, pp. 2748-2757.
6. Matsumoto, N. and Nairn, J. A., 2012, "Fracture Toughness of Wood and Wood Composites During Crack Propagation," Wood and Fiber Science, Vol. 44, pp. 121-133.
7. Nairn, J. A., 2009, "Analytical and Numerical Modeling of R Curves for Cracks with Bridging Zones," Int. J. Fracture, Vol. 155, pp. 167-181.
8. Bao G, and Suo Z, 1992, "Remarks on Crack-Bridging Concepts," Appl Mech Rev, Vol. 45, pp. 355–366.
9. ASTM Standard E399-05a: Standard Test Method for Plane-Strain Fracture Toughness of Metallic Materials, Annual Book of ASTM Standards, ASTM International, West Conshohocken, PA, 2006
10. Atack, D., May, W. D., Morris, E. L., and Sproule, R. N., 1961, "The Energy of Tensile and Cleavage Fracture of Black Spruce," Tappi, Vol. 44, pp. 555–567.
11. DeBaise, G. R., Porter, A. W., and Pentoney, R. E., 1966, "Morphology and Mechanics of Wood Fracture," Mat. Res. Stand., Vol. 6, pp. 493–499.
12. Schniewind, A. P. and Pozniak, R. A., 1971, "On the Fracture Toughness of Douglas Fir Wood," Engineering Fracture Mechanics, Vol. 2, No. 223–233.

13. Schniewind, A. P. . and Centeno, J. . C., 1973, “Fracture Toughness and Duration of Load Factor I. Six Principal Systems of Crack Propagation and the Duration Factor for Cracks Propagating Parallel to Grain,” Wood Fiber, Vol. 5, No. 152–159.
14. Johnson, J. A., 1973, “Crack Initiation in Wood Plates,” Wood Science, Vol. 6, pp. 151–158.
15. Niemz, P. and Diener, M., 1999, “Comparative Investigations for the Determination of Fracture Toughness at Timber Materials,” Holz als Roh- und Werkstoff, Vol. 57, pp. 222–224.
16. Conrad, M. P., Smith, G. D., and Fernlund, G., 2003, “Fracture of Solid Wood: A Review of Structure and Properties at Different Length Scales,” Wood and Fiber Science, Vol. 35, pp. 570–584.
17. Atkins, A. G. and Mai, Y. W., 1985, *Elastic and Plastic Fracture*, John Wiley & Sons, New York.
18. Haygreen, J. G., and Bowyer, J. L., 1996. *Forest Products and Wood Science: An Introduction*, Iowa State University Press, Ames, Iowa, USA.
19. Fruhmann, K., Reiterer, A., Tschegg, E. K., and Stanzl-Tschegg, S. S., 2002, “Fracture Characteristics of Wood under Mode I, Mode II and Mode III loading,” Philosophical Magazine A: Physics of Condensed Matter, Structure, Defects and Mechanical Properties, Vol. 82, pp. 3289–3298.
20. Reiterer A, Sinn G, Stanzl-Tschegg S, 2002, “Fracture Characteristics of Different Wood Species Under Mode I Loading Perpendicular to the Grain,” Materials Science and Engineering A, Vol. 332, pp. 29–36.
21. Reiterer A, Burgert I, Sinn G, Tschegg S, 2002, “The Radial Reinforcement of the Wood Structure and its Implication on Mechanical and Fracture Mechanical Properties - A Comparison Between two Tree Species,” Journal of Materials Science, Vol. 37, No. 935–940.
22. Gibson, L. J., and Ashby, M. F., 1997, *Cellular Solids: Structure and Properties*, Cambridge University Press, Cambridge, England.